

# Microwave-assisted reconstruction of Ni,Al hydrotalcite-like compounds

P. Benito<sup>1</sup>, I. Guinea, F.M. Labajos, V. Rives\*

*Departamento de Química Inorgánica, Universidad de Salamanca, 37008 Salamanca, Spain*

Received 20 November 2007; received in revised form 28 January 2008; accepted 4 February 2008

Available online 20 February 2008

## Abstract

The microwave-assisted reconstruction of Ni,Al hydrotalcite-like compounds (HTlcs) with Ni/Al molar ratios 2/1 and 3/1 has been studied. Mixed oxides obtained after calcination of the HTlcs are immersed in three different solutions containing carbonate, distilled water and an aqueous NH<sub>3</sub> solution, and then heated at different temperatures for increasing periods of time under microwave radiation. The evolution of the structure during the treatment is followed by powder X-ray diffraction, FT-IR and vis–UV spectroscopies and SEM and TEM microscopies. Full recovery of the original layered structure is achieved in short periods of time for the 2/1 samples when the calcined HTlcs are rehydrated in the Na<sub>2</sub>CO<sub>3</sub> solution, but more drastic conditions are necessary for the 3/1 samples and the reconstruction seems not to be complete. Finally, only a partial reconstruction is observed in distilled water or NH<sub>3</sub> aqueous solution. © 2008 Elsevier Inc. All rights reserved.

**Keywords:** Hydrotalcite-like compounds; Nickel; Reconstruction; Microwave; Hydrothermal

## 1. Introduction

Layered double hydroxides (LDHs) constitute a family of lamellar compounds built by the stacking of brucite-type layers where a partial substitution of the divalent cations has taken place; the positive charge is thereof balanced by introducing some anions in the interlamellar region, where they coexist with water molecules [1]. Calcination at ca. 500 °C gives rise to MgO-type, poorly crystallized, mixed oxides, which show high specific surface area values, high metallic dispersion and particle stability against sintering; for these reasons they have been widely applied as catalysts [2,3].

However, another well-known property of LDHs is their ability to recover the original layered structure after being calcined at different temperatures and then exposed to air or immersed in a solution containing different anions, the so-called “memory effect” [4]. Carbonate-containing hydrotalcite-like compounds (HTlcs) are usually used as

precursors for the reconstruction process. To overcome the high affinity of carbonate anions for the layers, which makes them unsuitable as anion-exchange precursors, the anions can be easily removed by thermal treatment. The most important factor required is the calcination temperature, which must be high enough to remove most of the interlayer anions. The main advantage of this method is the prevention of competitive intercalation of anions in HTlcs. In this way, it is possible to intercalate some anions in the interlamellar space from calcined carbonate-containing LDHs such as polyoxometalates [5], aminoacids [6], chromophores [7], carboxylate anions [8], dyes [9], etc. In addition, the reconstruction method is the easiest way to prepare the OH-intercalated phase, known as meixnerite, very active in base-catalyzed reactions, such as aldol, Knoevenagel and Claisen–Schmidt condensations and Michael additions in liquid phase under mild conditions [10–15]. Finally, other authors used this method to prepare catalysts. For instance, a Ni-loaded catalyst with an egg-shell shape was successfully prepared by adopting the memory effect of Mg–Al HTlcs: a Mg–Al mixed oxide was prepared by calcination of a Mg–Al hydrotalcite and then dipped in a Ni(II) nitrate aqueous solution [16].

\*Corresponding author. Fax: +34 923 29 45 74.

E-mail address: [vrives@usal.es](mailto:vrives@usal.es) (V. Rives).

<sup>1</sup>Present address: Dip. Chimica Industriale e dei Materiali, University of Bologna, Viale Risorgimento 4, 40136 Bologna, Italy.

The extent of the reconstruction process depends on several factors, such as the temperature and time of calcination and the number of times the LDH is calcined at a given calcination temperature and time (i.e., cycling treatments) [4,17,18]. Usually, full reconstruction is only observed for samples where the formation of well crystalline materials (e.g. spinels) has not been completed, although a partial rehydration to a layered structure has been reported for products calcined even at higher temperature ( $\leq 800$  °C) [18].

In addition, depending on the nature of the cations involved, total reconstruction requires different conditions [19], and it is even more complicated when more than two cations are present in the brucite-type layer [20]. For instance, Mg,Al mixed oxides easily recover their lamellar structure under rather mild conditions [4]. However, during reconstruction of Zn,Al hydrotalcites previously calcined at 300–400 °C, a second phase, aluminum hydroxide or zinc oxide, was generally detected, and a spinel phase, formed during calcination above 600 °C, inhibited reconstruction of the HT-like phase [21]. In the case of nickel-containing samples, severe conditions are needed for reconstruction, i.e. hydrothermal treatment for long periods of time, and even using high temperatures and pressures only a partial reconstruction is achieved [19,22,23]. Furthermore, the addition of  $\text{Ni}^{2+}$  cations to a Mg,Al compounds, reduces the ability of the oxide to recover the hydrotalcite structure [19]. Co-containing LDHs cannot be reconstructed even after thermal treatment at temperatures as low as 200 °C because of the formation of highly stable  $\text{Co}_3\text{O}_4$  spinel in an oxidant atmosphere [24]. However, reversible thermal behavior can be achieved if the calcination is performed in  $\text{N}_2$  atmosphere [25]. Finally, Mg,Fe oxides also reconstruct, but the efficiency of the reconstruction depends on the thermal annealing temperature and the Mg/Fe ratio [26].

The first studies carried out about the “memory effect” pointed out to a retrotopotactic mechanism [4]. However, the dissolution-recrystallization mechanism of hydrotalcite regeneration from mixed oxides has been recently accepted [19,26–29]. A deep study about the kinetics of the transformation using the nucleation-growth model of Avrami and Erofe'ev was carried out by Millange et al. [27] and then by Pérez-Ramirez et al. [19]. Using this model, it was assumed that the poorly crystalline mixed oxide dissolves in the sodium carbonate solution to give a concentrated solution of reactive species from which nucleation sites for the HTlc crystallization are formed. Other facts also supporting the dissolution–reprecipitation mechanism are the incorporation of other cations within the layers after exposing the oxides to a solution containing the cations [30], elimination of turbostratic disorder effects, and changes in the textural properties such as the particle shape [28]. Contrary, on the basis of experimental results (lack of morphological changes of the particles and of change of the XRD patterns) Delorme et al. [31] recently considered that the reconstruction process proceeds topotactically as previously proposed by Sato et al. [4].

Regarding the crystallinity of the original and reconstructed samples, different behaviors are found in the literature. While some authors report that there is no difference among them [20], others have found an enhancement of the crystallinity degree for the reconstructed samples [32,33], reducing the distortions in the octahedral arrangements of the coordinating atoms and average Al–O bond lengths [18,34]. In other cases a decrease of the crystallinity (with respect to samples prepared by the hydrothermal treatment) is observed; however, the crystallinity could be significantly improved if the last stage of the layered structure recovery is carried out in an autoclave [35]. Finally, Ulibarri et al. [36] also observed that a well-crystallized original LDH structure favors the reconstruction process. Regarding the polytype of the reconstructed HTlc, Stanimirova showed that the regenerated samples were always of 3R1 polytype, whichever the precursor structure [37]. On the other hand, Sychev and coworkers have shown that the reconstruction of calcined LDHs due to memory effect results in the formation of materials with different structures than those of the parent hydrotalcites [34].

Broadly speaking, two rehydration processes have been usually followed: gas-phase rehydration and liquid-phase rehydration. Several authors have compared the properties of the solids obtained by both methods [11,18,38–40]. They concluded that the textural properties of the samples strongly differ: the memory effect leads to a higher degree of reconstruction when rehydration is carried out in the gas phase, although liquid-phase rehydration under fast stirring produced larger surface area values.

In this work, we report for the first time full reconstruction of Ni,Al HTlcs in short periods of time under microwave-hydrothermal conditions. The study was carried out using two series of Ni,Al-HTs with molar Ni/Al ratios 2/1 and 3/1. The solids were calcined at moderate temperatures and subsequently were contacted with an aqueous  $\text{Na}_2\text{CO}_3$  solution, distilled water and an  $\text{NH}_3$  aqueous solution. In order to recover the original lamellar structure in short periods of time the solutions were heated in a microwave oven under hydrothermal conditions for several periods of time at different temperatures.

## 2. Experimental

### 2.1. Synthesis of the materials

Two series of Ni,Al- $\text{CO}_3$  HTlcs were synthesized by the coprecipitation method at constant pH, the Ni/Al molar ratios being 2/1 and 3/1, respectively. The slurry obtained was subsequently submitted to microwave-hydrothermal treatment for 300 min at 125 °C in a Milestone Ethos Plus microwave oven as reported elsewhere [41]. Calcined products were obtained by heating in air at 550 °C for 2 h, in the case of solids with a Ni/Al = 2/1, and at 450 and 550 °C for the 3/1 materials. The reconstruction process was carried out at several temperatures, i.e., 100, 125, 150

and 175 °C, for different periods of time under microwave-hydrothermal conditions. It was performed by dispersing the oxides, obtained after calcinations of 2 g of the HTlc, in 50 ml of a Na<sub>2</sub>CO<sub>3</sub> aqueous solution (pH = 12), in distilled and decarbonated water and in a NH<sub>3</sub>·H<sub>2</sub>O 1 wt.% aqueous solution (in this case the initial pH was 11, and after adding the calcined hydrotalcite it dropped until 10.5 owed to the weakness of the ammonium base and the reaction with the oxides and some CO<sub>2</sub> absorbed over the oxide surface). During the process the solutions were kept under continuous stirring in the microwave vessels. The microwave oven posses an ASM-400 Magnetic Stirring Module device in the bottom of the microwave cavity. An independently rotated magnet produces consistent stirring of solutions in all vessels, whichever their position within the cavity, when a stirring bar is introduced in the vessels.

The samples were named as follows: YNAHW300 and YNAHW300c for the precursor and the sample calcined at 550 °C, respectively; *Y* = 2 and 3 stands for the series with a molar Ni/Al ratio of 2/1 and 3/1, respectively. YNAcW-*T*-*t* is used for the reconstructed samples, where *T* is the heating temperature (125, 150 and 175 °C), and *t* stands for the irradiation time (10, 30, 60, 180 and 300 min). For the 3/1 samples calcined at 450 °C a digit 1 was added to the name, i.e. 3NAc1W-*T*-*t*.

## 2.2. Characterization techniques

Powder X-ray diffraction (PXRD) patterns were recorded in a Siemens D-500 instrument using CuK $\alpha$  radiation ( $\lambda = 1.54050 \text{ \AA}$ ) equipped with Diffrac AT software. The data were collected in the 5–70° ( $2\theta$ ) range with a 0.05° ( $2\theta$ ) step and a 1.5 s per step counting time. Identification of the crystalline phases was made by comparison with the JCPDS files [42]. The crystallite size was calculated by the Scherrer equation from the FWHM of the (003) and (006) using the Warren correction.

FT-IR spectra were recorded in a Perkin-Elmer FT1730 instrument, using KBr pellets; 100 spectra (recorded with a nominal resolution of 4 cm<sup>-1</sup>) were averaged to improve the signal-to-noise ratio.

UV-vis spectra were recorded following the diffuse reflectance (UV-vis/DR) technique in a Perkin-Elmer Lambda 35 instrument with a Labsphere RSA-PE-20 integrating sphere and software UV WinLab, using 2 nm slits and MgO as reference.

Specific surface area assessment was carried out in a Gemini instrument from Micromeritics. The sample (ca. 80–100 mg) was previously degassed in flowing nitrogen at 110 °C for 2 h in a FlowPrep 060 apparatus, also from Micromeritics, in order to remove physisorbed water, and the data were analyzed using published software [43]. The values of pore volume were obtained from the saturation adsorption capacities, the nitrogen uptake at  $p/p_0 = 0.950$  was converted into the adsorbed volume by assuming the adsorbate has the normal liquid density at the operational temperature.

The transmission and scanning electron photographs were taken at Servicio General de Microscopía Electrónica (University of Salamanca, Spain) with a ZEISS-902 Microscope. The samples were dispersed in acetone by ultrasounds, and some drops of this dispersion were deposited on a copper grid previously impregnated with an amorphous carbon film with a voltaic arc.

## 3. Results and discussion

### 3.1. 2/1 Carbonate intercalated samples

The PXRD patterns of the LDH precursor, 2NAHW300, calcined sample, 2NAHW300c, and reconstructed solids at 125 °C for different periods of time, 2NAcW-125-10, 2NAcW-125-30, 2NAcW-125-60, 2NAcW-125-180, 2NAcW-125-300, are shown in Fig. 1. The pattern for the original LDH, sample 2NAHW300, shows the typical reflections ascribed to HTlcs, symmetrical and intense reflections due to (003) and (006) diffraction planes at low  $2\theta$  and less intense and asymmetric reflections due to non basal planes at higher  $2\theta$ , together with the typical doublet close to 60–65° ( $2\theta$ ). This sample was submitted to microwave-hydrothermal treatment for 300 min at 125 °C to improve its crystallinity as reported elsewhere [44], since it has been shown that the different distributions of the cations in the LDH strongly affects the memory effect [36,45]. After thermal treatment at 550 °C, sample 2NAHW300c, the lamellar structure collapses and the only phase detected is a poorly crystallized cubic mixed-oxide NiO phase. The *a* cell parameter of the nickel oxide phase is 4.153 Å, slightly lower than that for pristine NiO, 4.177 Å, because of the inclusion of some Al<sup>3+</sup> cations with smaller ionic radius in the structure. However, according to Clause et al. this sample should be formed by three phases:

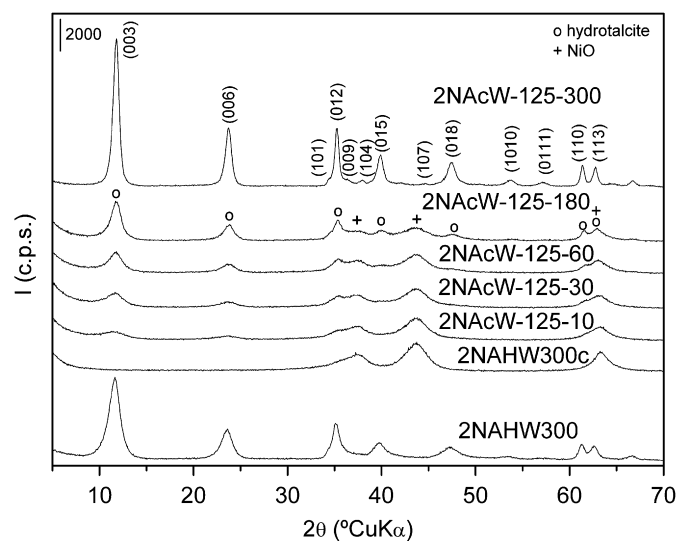


Fig. 1. PXRD patterns of the 2/1 precursor (2NAHW300), sample calcined at 550 °C (2NAHW300c) and samples reconstructed at 125 °C for 10, 30, 60, 180 and 300 min in the microwave suspended in a carbonate solution (2NAcW-125-10, 2NAcW-125-30, 2NAcW-125-60, 2NAcW-125-180 and 2NAcW-125-300, respectively).

a NiO phase probably containing  $\text{Al}^{3+}$  impurities, a spinel-type phase located on the surface of the NiO particles, and a nickel-doped  $\text{Al}_2\text{O}_3$  phase possibly graphed onto NiO and/or the spinel phase [46]. In other words, the NiO crystallites can be viewed as an oxide phase decorated by a spinel-type phase.

The evolution of the structure during the reconstruction process can be followed through the PXRD patterns. Just after 10 min of hydrothermal treatment under microwave radiation, sample 2NAcW-125-10, a hydrotalcite-type phase starts to appear, according to development of weak diffraction lines due to the basal planes. Upon submitting the samples to longer periods of time, samples 2NAcW-125-30, 2NAcW-125-60, 2NAcW-125-180, an increase in the intensity of the hydrotalcite-originated reflections is observed, while those due to the mixed oxides begin to vanish. Full recovery of the layered structure and total absence of the mixed oxide phase is only observed after 300 min irradiation, sample 2NAcW-125-300. Comparing the PXRD pattern of the original sample 2NAHW300, with that for sample 2NAcW-125-300, it is evident that an enhancement of the crystalline degree and removal of turbostratic disorder effects takes place during the reconstruction process (sharper and more intense peaks are recorded). Moreover, even weak diffraction peaks of the hydrotalcite-like phase, which are not recorded in the PXRD diagram of the original sample, 2NAHW300, can be seen in the pattern of the sample reconstructed during 300 min, sample 2NAcW-125-300. This fact is also supported by the increase in the crystallite size, see Table 1, from 60 Å for the original sample to 120 Å for the one reconstructed for 300 min.

The effect of the temperature during the reconstruction step on the crystallinity of the samples is also studied; the selected temperatures are 150 and 175 °C, 2NAcW-150 and 2NAcW-175 series, in addition to 125 °C, see E.S.I. information. When the irradiation temperature is in-

creased, a decrease in the time required to fully recover the layered structure is observed, as well as an improvement in the crystallinity degree with respect to the sample fully reconstructed at 125 °C, sample 2NAcW-125-300. Although the layered structure is not completely recovered after rehydration for 60 min at 150 °C, sample 2NAcW-150-60, recovering of the structure is complete when the treatment time is extended to 180 min, sample 2NAcW-150-180. Full recovery is achieved in only 60 min at 175 °C, sample 2NAcW-175-60. Table 1 summarizes the calculated average crystallite sizes for the final products under each reconstruction conditions studied. It is clear that, for a given reconstruction temperature the crystallite size of the reconstructed LDH increases with time, while the size also increases with temperature at a constant reaction time.

The higher crystallinity of the reconstructed materials can be related to two facts. If a topotactic reconstruction process is assumed, the memory method would lead to an increased degree of crystallinity, compared to that for the parent LDH, because of metal cations are still homogeneously dispersed in the mixed oxides formed upon calcination. Alternatively, the enhancement in crystallinity can be also due to the microwave treatment, similar to that observed during the ageing treatment [44].

Unit cell parameters,  $a$  and  $c$ , are also modified along the reconstruction process, Table 1. The  $c$  parameter is calculated assuming a 3R1 polytype, since no different polytypes are obtained, from the positions of the (003) and (006) reflection lines, using the formula  $c = 3[1/2(d_{(003)} + 2d_{(006)})]$  [47]. The unit cell parameters of the parent LDH sample, 2NAHW300, are also included in this table. A decrease in the value of the  $c$  parameter is observed for samples reconstructed at 125 °C as the irradiation time is increased and a pure LDH phase is formed. However, except for some of the samples, when the treatment temperature is increased to 150 °C the  $c$  cell parameter increases as well, the largest values being calculated for the series treated at 175 °C. These values are, however, always smaller than that calculated for the coprecipitated and microwave aged sample, 2NAHW300. The variations in the values here reported can be related to a modification of the interlayer composition, on the interlayer order [48] and the chemical composition.

The cell parameter  $a$  is calculated from position of the  $d_{(110)}$  reflection, the first peak of the doublet close to 60–65° ( $2\theta$ ),  $a = 2d_{(110)}$  [47]. The value of parameter  $a$  was lower for the not fully rehydrated samples, 2NAcW-125-30, 2NAcW-125-60, 2NAcW-125-180, than that for the original LDH, 2NAHW300; however, a steady increase in its value was observed with both temperature and microwave-hydrothermal treatment, reaching a value very close to the calculated for the starting LDH material, 3.02 Å for 2NAcW-125-300 sample. This parameter is related to the layer composition, as it depends on the ionic radii of the cations existing in the brucite-like layers.

Vis–UV spectra of the reconstructed samples also gives evidences about the reconstruction degree since the spectra

Table 1

Cell parameters,  $a$  and  $c$  (Å), and crystallite size ( $D$ , Å) of the 2/1 Ni,Al samples: precursor (NAHW300) and microwave-assisted reconstructed samples under different experimental conditions

Sample	$c$	$a$	$D$ (003)
2NAHW300	22.76	3.020	60
2NAcW-125-10	22.98	–	40
2NAcW-125-30	22.64	3.003	53
2NAcW-125-60	22.60	3.003	60
2NAcW-125-180	22.54	3.007	70
2NAcW-125-300	22.49	3.016	120
2NAcW-150-60	22.51	3.020	100
2NAcW-150-180	22.56	3.020	140
2NAcW-150-300	22.57	3.020	180
2NAcW-175-60	22.73	3.030	180
2NAcW-175-120	22.67	3.050	190

2NAHW300: original sample; 2NAcW- $T$ - $t$ : samples reconstructed at ( $T = 125, 150$  and  $175$  °C) for different periods of time ( $t = \text{min}$ ).

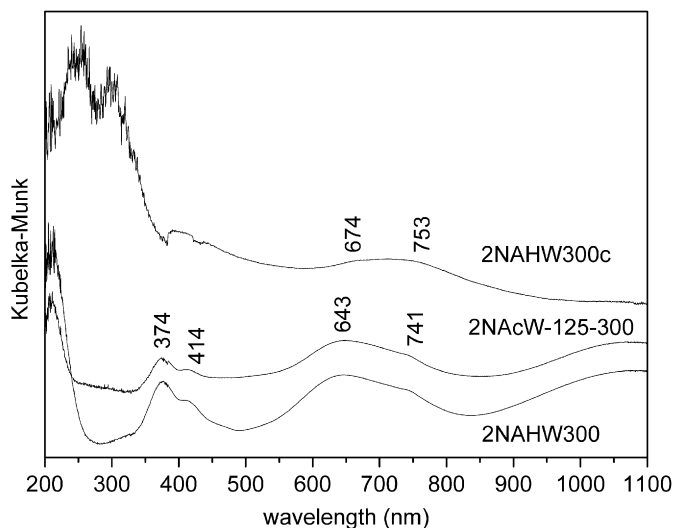


Fig. 2. Comparison between the vis-UV/DR spectra of the precursor, NAHW300, the sample calcined at 550 °C, NAHW300c, and the sample reconstructed at 125 °C for 300 min, 2NAcW-125-300.

of transition metal cations are very sensitive to their oxidation state and environment. A detailed description of the vis-UV spectra of Ni,Al-HTs and derivate oxides is given elsewhere [49]. Ni,Al-HTs show three bands around 450, 650 and 1150 nm, with shoulders at ca. 380 and 735 nm. For the mixed oxides, it should be here remarked the presence of some  $\text{Ni}^{2+}$  ions in tetrahedral holes, together with  $\text{Ni}^{2+}$  in octahedral ones, and of  $\text{Ni}^{3+}$  species in the oxides obtained by calcination at 550 °C, responsible for the intense background and intense charge transfer band in the ultraviolet region. The vis-UV spectra of the microwave-hydrothermally treated samples show that Ni ions recovered their original location in octahedral holes, Fig. 2, and that this relocation is complete after 300 min treatment, sample 2NAcW-125-300; the band at lower wavelength almost disappears and the broad absorption due to  $\text{Ni}^{3+}$  ions is almost negligible; actually, the sample recovered its original green color. The same behavior is observed for the solids reconstructed at higher temperatures, NA2cW-150 and NA2cW-175 series.

Recovering of the structure can be also assessed by the evolution of the characteristic infrared bands of the hydrotalcite structure [50]. FT-IR spectra of the 2/1 samples reconstructed at 125 °C during increasing periods of time are shown in Fig. 3. The main changes are observed in the 1400–1200  $\text{cm}^{-1}$  region and in the low wavenumber region; the bands due to hydroxyl groups (3800–3000  $\text{cm}^{-1}$ ) and water molecules (ca. 1630  $\text{cm}^{-1}$ ) do not change appreciably. Carbonate anions existing in the solution are steadily incorporated during the reconstruction process into the structure, as it is confirmed by the progressive increase in the intensity of the band at ca. 1365  $\text{cm}^{-1}$ , attributed to the  $\nu_3(\text{CO}_3)$  mode. On the other hand, only weak bands characteristic of the oxides vibrations are recorded in the low wave number region for the sample irradiated for shorter periods of time;

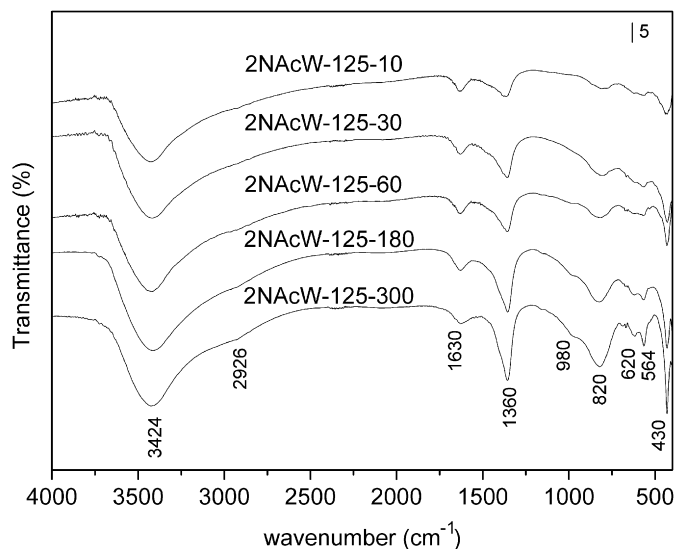


Fig. 3. FT-IR spectra of 2/1 samples reconstructed at 125 °C during increasing periods of time: 10 min (2NAcW-125-10), 30 min (2NAcW-125-30), 60 min (2NAcW-125-60), 180 min (2NAcW-125-180), and 300 min (2NAcW-125-300).

however, when the original structure is fully recovered, intense and well-defined FTIR bands are observed: the shoulder at ca. 980  $\text{cm}^{-1}$  is due to the  $\nu_{\text{def}}$  Al-OH; the peak at ca. 564  $\text{cm}^{-1}$  is due to the Al-OH translational mode; the sharp and intense band at ca. 430  $\text{cm}^{-1}$  has been attributed to a condensed  $[\text{AlO}_6]^{3-}$  group or as single Al-O bonds; the bands due to the  $\nu_2$  and  $\nu_4$  carbonate vibration modes are observed in the infrared spectrum at 820 and 694  $\text{cm}^{-1}$ ; and finally, the peak at 620  $\text{cm}^{-1}$  might be related to the presence of Ni cations, Ni-OH translation [50]. In addition, the broad band due to  $\nu_{\text{OH}}$  vibration at higher wavenumber, due to OH stretching mode of hydroxyl and water molecules, becomes narrower along the treatment time, and the shoulder recorded at ca. 2900  $\text{cm}^{-1}$ , due to the interaction between interlamellar water molecules and carbonate anions, gains intensity as well, pointing to a higher intralamellar order for the reconstructed samples. When the reaction temperature is increased the FT-IR spectra (not shown) are better defined, as a consequence of a better-ordered structure.

The textural properties (i.e., specific surface area, pore volume, and average pore size) of selected reconstructed solids, 2NAcW-125-300, 2NAcW-150-180 and 2NAcW-150-300, 2NAcW-175-60 and 2NAcW-175-120, are analyzed by  $\text{N}_2$  adsorption/desorption at -196 °C, and they are compared to those of the lamellar precursor, 2NAHW300, and of the calcined product, 2NAHW300c. All solids show isotherms characteristics of this kind of compounds, type IIb in the classification given by Rouquerol [51]. The only differences found between them are related to the decrease of the width of the hysteresis loop, characteristic of a well-defined pore size distribution. Clear differences are observed among the BJH plots of the samples before and after calcination, 2NAHW300 and

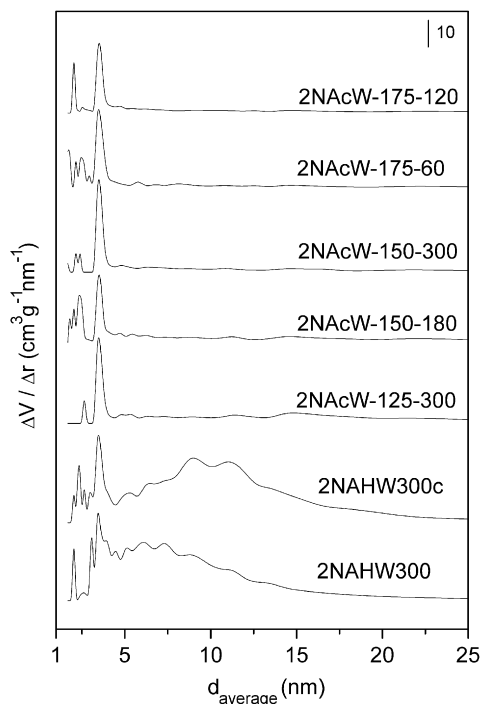


Fig. 4. Pore size distribution plots of the 2/1 Ni,Al-CO<sub>3</sub> fully reconstructed samples.

2NAHW300c, and after reconstruction, 2NAcW-125-300, 2NAcW-150-180, 2NAcW-150-300, 2NAcW-175-60 and 2NAcW-175-120 (Fig. 4). The original sample, 2NAHW300, shows pores with a diameter close to 4 nm, together with a broad pore size distribution of larger mesopores. Due to the cratering mechanism, new mesopores with larger diameter are created after calcinations, sample 2NAHW300c. The large mesopores disappear in the rehydrated solids and all they show a quite similar narrow pore size distribution. Consequently, it can be stated that the microwave-assisted reconstruction process leads to a cancellation of the larger pores and mainly pores ranging 3–4 nm exist in the reconstructed solids, although a contribution from smaller pores is also observed in the plots. These differences can be attributed to the modification of the particle size and shape [41], see electronic microscopy results below.

The  $S_{\text{BET}}$  and  $V_p$  values for the fully reconstructed 2/1 samples, together with the data for the precursor and for calcined compound, are summarized in Table 2. The as-synthesized sample 2NAHW300, displays a specific surface area around  $150 \text{ m}^2 \text{ g}^{-1}$ , this value (as well as the pore volume) increases after calcination. The specific surface areas measured for the reconstructed samples are always smaller; furthermore, the  $S_{\text{BET}}$  and  $V_p$  values decrease whenever the irradiation time and the temperature are increased, a feature also related to the crystalline degree of the solids. In previous works, Abelló and coworkers have observed that rehydration of MgAl LDHs in the liquid phase by mechanical stirring [39] or ultrasounds [52] produced an increase in the surface area due to rupture of particles and a marked exfoliation of the crystals.

Table 2

$S_{\text{BET}}$  specific surface areas ( $\text{m}^2 \text{ g}^{-1}$ ) and pore volume ( $\text{ml g}^{-1}$ ) for the precursor, the calcined sample and the microwave-assisted fully reconstructed samples

Sample	$S_{\text{BET}}$	$V_p$
2NAHW300	147	0.444
2NAHW300c	197	0.678
2NAcW-125-300	69	0.275
2NAcW-150-180	60	0.194
2NAcW-150-300	43	0.127
2NAcW-175-60	44	0.130
2NAcW-175-120	35	0.097

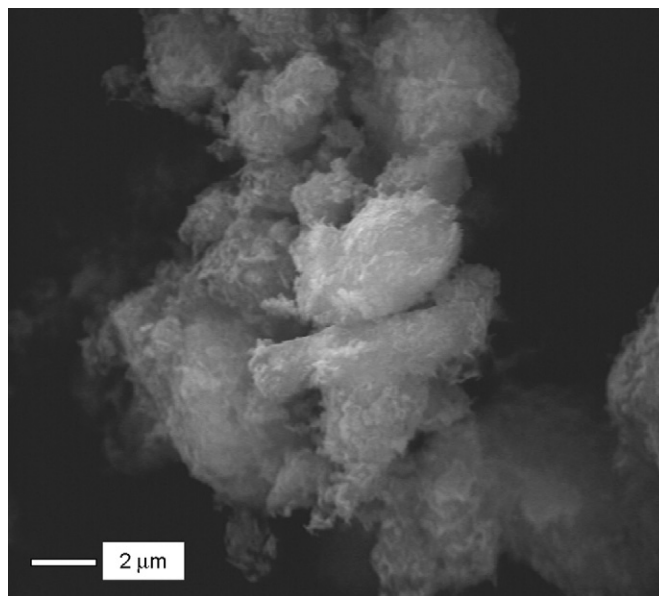


Fig. 5. SEM image of sample 2NAcW-125-300.

However, in the work here reported, the lower specific surface area of the rehydrated solids and the further cancellation of the porosity under more severe reconstruction conditions can be related to the crystalline degree of the reconstructed solids and to a dissolution and precipitation process of the LDHs once the structure has been rehydrated. The largest crystallinity is generally related to larger particles with a lower surface/mass ratio, as it will be confirmed by electronic microscopy (see below). However, it should be noticed that sample NA2cW-125-300 shows a rather large  $S_{\text{BET}}$  value in comparison to its high crystalline degree, which may be ascribed to the rapid heating achieved by the use of microwave radiation [41].

The morphology of the reconstructed samples is studied by SEM and TEM microscopy. SEM image of sample 2NAcW-125-300 is displayed in Fig. 5. Whenever the rehydration is performed at 125 or at 150 °C for 300 min, the shape of the particles is similar to that of other LDHs; agglomerates of plate-like particles, whose size depends on the reconstruction temperature; larger particles

are observed for the compound obtained at 150 °C (not shown), in agreement with results above commented.

More detailed information about the shape of single particles is obtained by TEM microscopy. The electron micrography of the sample obtained in 300 min at 125 °C, 2NAcW125-300, Fig. 6a, evidences a broad particle size distribution of particles with a non-regular shape, although some hexagonal platelets with rounded edges can be observed. In addition, some fibrous particles, characteristic of takovite compounds, are present as well. When the heating temperature is 150 °C along 180 min, sample 2NAcW-150-180 (not shown), some fibrous particles are still observed, but a similar particle size and shape distribution as for the sample heated at 125 °C for 300 min is observed. Conversely, for sample 2NAcW-150-300, Fig. 6b, a more homogeneous distribution of better defined and larger hexagonal particles is observed. Finally, for the samples obtained at the highest temperatures (not shown), no further improvements are achieved, although the crystallinity of these compounds was considerably better.

However, taking into account the well-crystallized compound obtained by this method and the advantages of homogenous heating because of the use of microwaves, a more homogeneous distribution of well-defined hexagonal platelets should have been obtained. On the other hand, these results are in agreement with those previously reported for reconstructed samples that had lost their original hexagonal shape [17]. This change is attributed to the effect of the mechanical stirring during the reconstruction process, which can break the hydroxalcite-like platelets [39].

### 3.2. 2/1 OH intercalated samples

After successful reconstruction of Ni,Al-CO<sub>3</sub> compounds in really short periods of time, the reconstruction of Ni,Al HTlcs in distilled water is studied in order to obtain OH intercalated compounds by using the microwave-assisted reconstruction method. In previous works it was not possible to fully recover the original lamellar structure under these conditions, even though the recon-

struction was carried out under hydrothermal treatment at high temperatures [33].

Several attempts are made in order to restore under the meixnerite-like form the Ni-containing mixed oxides in this work, but contrary to the carbonate intercalated compounds, their rehydroxylation into the lamellar structure hardly occurs. It was impossible to fully reconstruct the hydroxalcite compound previously calcined at 550 °C, NiO phase reflection lines are always observed in the diffraction patterns despite the increase of irradiation time and temperature (data not shown). Moreover, two new phases are identified, boehmite and bayerite, which are formed from amorphous alumina on the surface of the NiO crystals, i.e. coming from Al-doped particles [22,53]. The presence of this minor phase indicates that hydrothermal treatments in distilled water produces boehmite in a first stage and then Ni,Al hydroxalcite [23]. The different behavior between the reconstruction in distilled water and in an aqueous sodium carbonate solution can be related to the lower pH of the solution, too low to permit precipitation of hydroxalcite or redissolution of the segregated aluminum species and NiO and their further re-incorporation to the hydroxalcite structure.

Even if the calcination temperature is lowered at 450 °C (data not shown), no enhancement of the degree of reconstruction is observed. However, the amount of boehmite side-phase is considerably decreased. The calcination temperature is one of the main factors that determine the segregation of an aluminum side phase to form the NiO-decorated aluminate-type patches; for this reason, by decreasing the calcination temperature ca. 100 °C, the segregation is partially cancelled, so when the oxide is immersed in water and irradiated for 120 min at 175 °C, sample NAcW-175-120, only small reflections of boehmite are detected by PXRD. Consequently, it can be concluded that the microwave radiation does not allow to fully recovering the original lamellar structure when only water is used as solution.

As a final point, when the reconstruction process to obtain a hydroxyl-intercalated compound is performed in

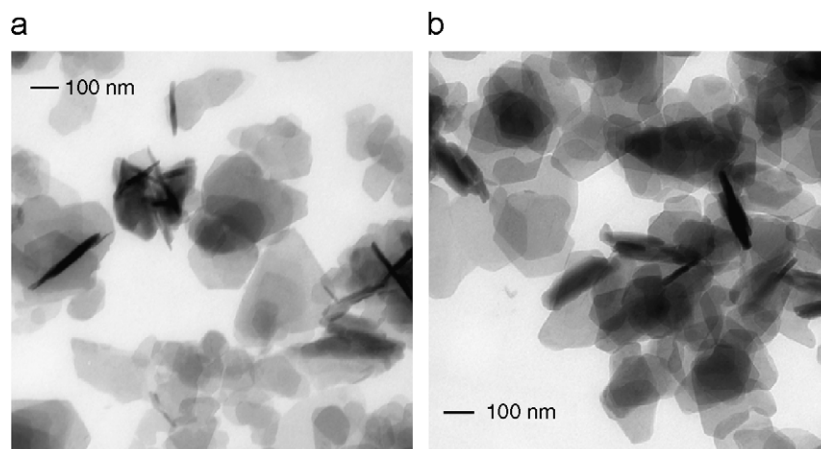


Fig. 6. TEM micrograph of sample 2NAcW-125-300 (a) and 2NAcW-150-300 (b).

an ammonia solution, although the reconstruction yield is improved, i.e., it was possible to achieve a partial recovery of the lamellar structure at 125 °C for 300 min, no full reconstruction was attained under all the reconstruction conditions. The same behavior is observed by decreasing the calcination temperature, although in this case no side phase is observed, because of the lower aluminum segregation and the higher pH of the original NH<sub>3</sub> solution in comparison with distilled water.

### 3.3. 3/1 Carbonate intercalated samples

Regarding the 3/1 series of samples, the behavior observed is slightly different, see Fig. 7. When the reconstruction is performed at 125 °C for 300 min (sample 3NAcW-125-300), some Ni<sup>2+</sup> and/or Al<sup>3+</sup> could not be transformed back to the original hydrotalcite-type structure and some peaks due to the NiO phase are still observed between 30–60° (2θ). Neither increasing the irradiation time nor the heating temperature yields the full reconstruction; in all cases NiO diffraction lines are observed. However, it should be stressed that no reflections due to any aluminum compound (oxide or hydroxide) are observed in the diffraction patterns, although the formation of some amorphous alumina cannot be ruled out. Furthermore, it should be remarked that reconstructed samples always display a blackish color; this fact points to the existence of some residual Ni<sup>3+</sup> in the final structure in a non-stoichiometric NiO-type phase, confirmed by vis–UV spectra (not shown).

In order to avoid the spinel formation, a portion of the starting LDH is calcined at a lower temperature, i.e. 450 °C (samples 3NAc1W-*T-t*). Upon reconstruction under microwave irradiation, the hydrotalcite-like phase is almost fully recovered at 125 °C, but with some residual oxide phase.

Higher temperatures leads to regeneration of the layered structure in shorter periods of time and the PXRD patterns do not give any evidence about the presence of some residual oxide phase. However, vis–UV spectra confirm still the presence of some Ni<sup>2+</sup> cations outside of the brucite-type layers, Fig. 8, that are not detectable by PXRD.

### 3.4. Discussion

The results here reported clearly demonstrate that the microwave-assisted reconstruction of Ni,Al LDHs depends on the formulation of the parent compound and on the decomposition temperature, as well as on the reconstruction conditions, i.e. temperature and irradiation time. Full reconstruction is easily achievable for the 2/1 series in a

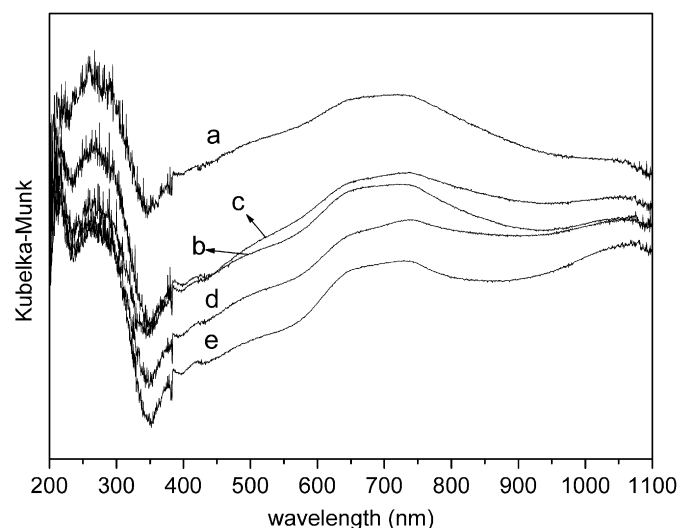


Fig. 8. DR/vis–UV spectra of 3NAc1W-125-300 (a), 3NAc1W-150-180 (b), 3NAc1W-150-300 (c), 3NAc1W-175-180 (d), 3NAc1W-175-300 (e).

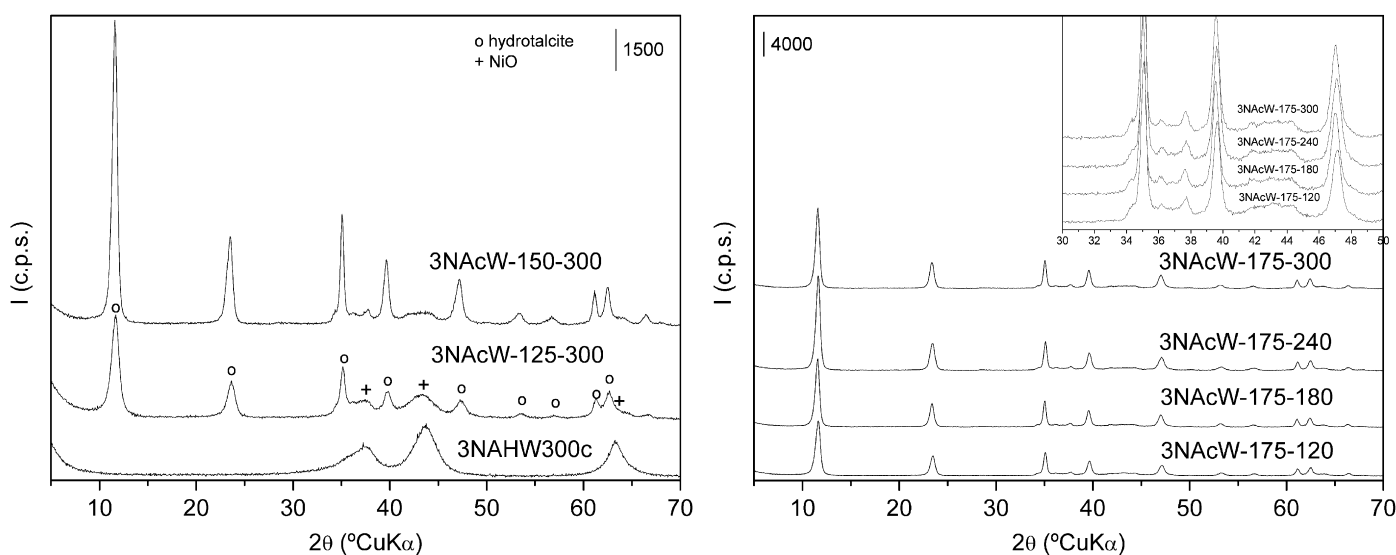


Fig. 7. PXRD patterns of the 3/1 samples reconstructed: (left) at 125 and 150 °C for 300 min 3NAcW-125-300 and 3NAcW-150-300, respectively; (right) at 175 °C for 120 (3NAcW-175-120), 180 (3NAcW-175-180), 240 (3NAcW-175-240) and 300 min (3NAcW-175-300).



$\text{Na}_2\text{CO}_3$  solution. On the other hand, only partial rehydration is attained by suspending the oxide in distilled water, and an improvement of the reconstruction yield is only observed when it is performed in an ammonia solution. Finally, when the molar ratio is 3/1 the rehydration process is delayed.

The reconstruction of Ni,Al oxides obtained by calcination of HTLcs can be easily achieved under microwave-hydrothermal treatment for compounds with a 2/1 ratio, whenever a strong basic media is used. Assuming the dissolution-precipitation mechanism is the responsible of the reconstruction of the LDHs, microwave radiation can improve the dissolution process of the oxide or hydroxide phases, improving the reconstruction in comparison to results previously reported by using a conventional hydrothermal treatment. This feature can be related to the formation of “active water molecules” [54], enhancing also the formation of nucleation sites and by interacting with the ions and increasing their mobility it can also improve the diffusion of the reactive species through the solution to the site of crystallization, a crucial step during the crystallization of the LDHs [27]. However, the microwave radiation cannot overcome the problems concerning the pH required to successfully solve the phases formed after calcinations. When using water, it is not possible to dissolve NiO and the segregated alumina species, so the reconstruction is reduced; however in an  $\text{NH}_3(\text{aq})$  solution both the solubility of nickel oxide and alumina particles is enhanced, but the structure is still not fully recovered. It seems that the presence of carbonate also favors reconstruction, i.e., formation of the carbonate-intercalated compound (the most stable from a thermodynamic point of view) is mostly favored in comparison with formation of meixnerite.

When the Ni/Al ratio is increased, the limited reconstruction observed can be related to the formation of spinel phases and the dissolution process, which are intimately related. The spinel formation should be decreased because of the low amount of aluminum cations; however, previous results have demonstrated that under cycling treatments the segregation of the spinel phase is favored when increasing the Ni/Al ratio [17], for this reason full reconstruction process only takes place for solids calcined below 300 °C, as below this temperature the  $\text{Al}^{3+}$  cations still remain dissolved within the NiO phase and no  $\text{Al}^{3+}$  migration to the surface, which would hinder reconstruction of the layers, has taken place [5]. In this situation, it would seem that because of a larger amount of nickel, the nickel oxide is more crystalline and larger particles are formed, increasing the segregation of aluminum outside the oxide phase and decreasing the amount of metastable phase,  $\text{Ni}_{1-x}\text{Al}_{2x/3}\delta_{x/3}\text{O}$  widely accepted as the responsible of the memory effect. This metastable phase tries to achieve stability or by forming the spinel phase or by reverting back to the parent LDH structure by dissolution [55]. However, if a quite crystalline NiO phase is formed with larger crystallite and particle sizes it should show a poorer

solubility than the mixed oxide, and for this reason the calcination must be performed at lower temperatures, since the presence of the metastable phase seems to be necessary to increase the solubility of the oxide. In fact, very recently, a method to kinetically stabilize the metastable oxide MgAl oxide with an amorphous phosphate network has been proposed and it was shown that it was possible to recover the structure even after calcinations at quite high temperatures [55].

#### 4. Conclusions

The use of microwave radiation as a heating source allows to enhance the kinetics of reconstruction of Ni,Al- $\text{CO}_3$ , because of an improved dissolution-precipitation process, when the Ni/Al ratio is 2/1 and the process is performed by contacting the mixed oxide with a  $\text{Na}_2\text{CO}_3$  solution. However, when a larger Ni/Al ratio is used or the process is carried out in water or in an aqueous  $\text{NH}_3$  solution, no successful results were obtained.

#### Acknowledgments

The authors thank financial support from MCyT (Grant MAT2006-10800-C02-01), Fundación Samuel Solorzano, JCyL (Grant SA030/03) and ERDF. A grant from JCyL to PB is acknowledged.

#### Appendix A. Supporting information

Supplementary data associated with this article can be found in the online version at doi:10.1016/j.jssc.2008.02.003.

#### References

- [1] V. Rives, Layered Double Hydroxides: Present and Future, Nova Science, New York, 2001.
- [2] D. Tichit, B. Coq, *Cattech* 7 (2003) 206–217.
- [3] S. Albertazzi, F. Basile, A. Vaccari, Catalytic properties of layered double hydroxides clay surfaces, in: F. Wypych (Ed.), *Fundamentals and Applications*, Elsevier, Amsterdam, 2004, pp. 497–546.
- [4] T. Sato, H. Fujita, T. Endo, M. Shimada, A. Tsunashima, *React. Solids* 5 (1988) 219–228.
- [5] F. Kooli, V. Rives, M.A. Ulibarri, *Inorg. Chem.* 34 (1995) 5114–5121.
- [6] H. Nakayama, N. Wada, M. Tshako, *Int. J. Pharm.* 269 (2004) 469–478.
- [7] G.G. Aloisi, U. Costantino, F. Elisei, L. Latterini, C. Natalia, M. Nocchetti, *J. Mater. Chem.* 12 (2002) 3316–3323.
- [8] L.P. Cardoso, J.B. Valim, *J. Phys. Chem. Solids* 65 (2004) 481–485.
- [9] H. Laguna, S. Loera, I.A. Ibarra, E. Lima, M.A. Vera, V. Lara, *Micropor. Mesopor. Mater.* 98 (2007) 234–241.
- [10] B. Choudary, M. Lantam, C. Reddy, K. Rao, F. Figueras, *J. Mol. Catal. A Chem.* 146 (1999) 279–284.
- [11] M. Climent, A. Corma, S. Iborra, A. Velty, *Catal. Lett.* 79 (2002) 157–163.
- [12] K. Rao, M. Gravelle, J. Sanchez Valente, F. Figueras, *J. Catal.* 173 (1998) 115–121.
- [13] M. Climent, A. Corma, S. Iborra, A. Velty, *J. Catal.* 221 (2004) 474–482.

- [14] J. Roelofs, J. van Dillen, P. de Jong, *Catal. Today* 60 (2000) 297–303.
- [15] S. Abello, F. Medina, D. Tichit, J. Pérez-Ramírez, J.E. Sueiras, P. Salagre, Y. Cesteros, *Appl. Catal. B Environ.* 70 (2007) 577–584.
- [16] K. Takehira, T. Shishido, D. Shouro, K. Murakami, M. Honda, T. Kawabata, K. Takaki, *J. Catal.* 231 (2005) 92–104.
- [17] T. Hibino, A. Tsunashima, *Chem. Mater.* 10 (1998) 4055–4061.
- [18] J. Rocha, M. del Arco, V. Rives, M.A. Ulibarri, *J. Mater. Chem.* 9 (1999) 2499–2503.
- [19] J. Pérez-Ramírez, S. Abello, N.M. van der Pers, *J. Phys. Chem. C* 111 (2007) 3642–3650.
- [20] N. Das, A. Samal, *Micropor. Mesopor. Mater.* 72 (2004) 219–225.
- [21] F. Kooli, C. Depège, A. Ennaqadi, A. de Roy, J.P. Besse, *Clays Clay Miner.* 45 (1997) 92–98.
- [22] B. Rebours, J.B. d’Espinoise de la Caillerie, O. Clause, *J. Am. Chem. Soc.* 116 (1994) 1707–1717.
- [23] F. Prinetto, G. Ghiotti, P. Graffin, D. Tichit, *Micropor. Mesopor. Mater.* 39 (2000) 229–247.
- [24] J. Pérez-Ramírez, G. Mul, F. Kapteijn, J. Moulin, *Mater. Res. Bull.* 36 (2001) 1767–1775.
- [25] A.V. Radha, G.S. Thomas, P.V. Kamath, C. Shivakumara, *J. Phys. Chem. B* 111 (2007) 3384–3390.
- [26] O.P. Ferreira, O.L. Alves, D.X. Gouveia, A.G. Souza Filho, J.A.C. de Paiva, J. Mendes Filho, *J. Solid State Chem.* 177 (2004) 3058–3069.
- [27] F. Millange, R.I. Walton, D. O’Hare, *J. Mater. Chem.* 10 (2000) 1713–1720.
- [28] M. Rajamathi, G.D. Nataraja, S. Ananthamurthy, P. Vishnu Kamath, *J. Mater. Chem.* 10 (2000) 2754–2757.
- [29] S. Stanimirova, G. Kirov, E. Dinolova, *J. Mater. Sci. Lett.* 20 (2001) 453–455.
- [30] S.K. Jana, Y. Kubota, T. Tatsumi, *J. Catal.* 247 (2007) 214–222.
- [31] F. Delorme, A. Seron, M. Bizi, V. Jean-Prost, D. Martineau, *J. Mater. Sci.* 41 (2006) 4876–4882.
- [32] I. Melián-Cabrera, M. López Granados, J.L.G. Fierro, *Catal. Lett.* 84 (2002) 3–4.
- [33] F. Pinetto, D. Tichit, R. Teissier, B. Coq, *Catal. Today* 55 (2000) 103–116.
- [34] M. Sychev, R. Prihod’ko, K. Erdmann, A. Mangel, R.A. van Santen, *Appl. Clay Sci.* 18 (2001) 103–110.
- [35] R.P. Bontchev, S. Liu, J.L. Krumhansl, J. Voigt, T.M. Nenoff, *Chem. Mater.* 15 (2003) 3669–3675.
- [36] M.A. Ulibarri, I. Pavlovic, C. Barriga, M.C. Hermosin, J. Cornejo, *Appl. Clay Sci.* 18 (2001) 17–27.
- [37] T. Stanimirova, G. Kirov, *Appl. Clay Sci.* 22 (2003) 295–301.
- [38] M. Climent, A. Corma, S. Iborra, A. Vely, *Green Chem.* 4 (2002) 474–480.
- [39] S. Abelló, F. Medina, D. Tichit, J. Pérez-Ramírez, J.C. Groen, J.E. Sueiras, P. Salagre, Y. Cesteros, *Chem. Eur. J.* 11 (2005) 728–739.
- [40] J.C.A.A. Roelofs, D.J. Lensveld, A.J. van Dillen, K.P. de Jong, *J. Catal.* 203 (2001) 184–191.
- [41] P. Benito, F.M. Labajos, J. Rocha, V. Rives, *Micropor. Mesopor. Mater.* 94 (2006) 148–158.
- [42] JCPDS, Joint Committee on Powder Diffraction Standards, International Centre for Diffraction Data, Swarthmore, PA, 1977.
- [43] V. Rives, *Adsorption Sci. Technol.* 8 (1991) 95–104.
- [44] P. Benito, F.M. Labajos, V. Rives, *J. Solid State Chem.* 179 (2006) 3784–3797.
- [45] V. Davila, E. Lima, S. Bulbulian, P. Bosch, *Micropor. Mesopor. Mater.* 107 (2008) 240–246.
- [46] O. Clause, B. Rebours, E. Merlen, F. Trifirò, A. Vaccari, *J. Catal.* 133 (1992) 231–246.
- [47] F. Cavani, F. Trifirò, A. Vaccari, *Catal. Today* 11 (1991) 173–301.
- [48] F.M. Labajos, V. Rives, M.A. Ulibarri, *J. Mater. Sci.* 27 (1992) 1546–1552.
- [49] M.J. Holgado, V. Rives, M.S. San Román, *Appl. Catal. A Gen.* 214 (2001) 219–228.
- [50] J.T. Klopogge, R.L. Frost, Layered double hydroxides, in: V. Rives (Ed.), *Present and Future*, Nova Science Publishers, Inc., New York, 2001, p. 139.
- [51] F. Rouquerol, J. Rouquerol, K. Sing, in: *Adsorption by Powders and Porous Solids. Principles, Methodology and Applications*, Academic Press, London, 1999.
- [52] S. Abelló, F. Medina, D. Tichit, J. Pérez-Ramírez, Y. Cesteros, P. Salagre, J.E. Sueiras, *Chem. Commun.* (2005) 1453.
- [53] O. Lebedeva, D. Tichit, B. Coq, *Appl. Catal. A Gen.* 183 (1999) 61–71.
- [54] M.C.R. Symons, *Acc. Chem. Res.* 14 (1981) 179–187.
- [55] A.V. Radha, P. Vishnu Kamath, N. Ravishankar, C. Shivakumara, *Langmuir* 23 (2007) 7700–7706.